Design and Structural Analysis of A Quadrotor

Mohd Ehsanul Hafizi Daud, Mohd Shariff Ammoo*, Iskandar Shah Ishak, Shabudin Mat

Department of Aeronautics, Automotive and Ocean Engineering
School of Mechanical Engineering, Faculty of Engineering
Universiti Teknologi Malaysia
81310 UTM Johor Bahru
Johor, Malaysia

ABSTRACT

This paper summarizes the design works and structural analysis that have been carried out on a single-seat electrical powered quadrotor or quadcopter as it is sometimes known. Using SolidWorks software, a number of designs were successfully developed by reverse engineering technique of the FURIA helicopter's design. The critical components of the selected design were analyzed using ABAQUS software for the static and dynamic loadings. Subsequently, the analyses provide a means of proposing a lightweight design efficaciously but yet strong enough to sustain the applied loads. As for the suspension system, the analysis was done through MATLAB and the best values for the spring constant, k and the damping coefficient, c to be used in this quadrotor system have been successfully quantified

Keywords: *Design, helicopter, quadrotor, structural analysis*

1.0 INTRODUCTION

The application of quadrotor (or quadcopter) in unmanned aerial vehicle (UAV) is limitless nowadays due to its simplicity, mainly in term of construction and maintenance and also its capability to take off and landing vertically [1]. This particular aircraft is well known as quadrotor helicopters and their mission concept varies, ranging from basic social purposes such as recreational, hobbyist and photography to military missions, which are more advanced and delicate. Literally, the term "quadrotor" means four rotors, consisting of two pairs of counter-rotating, fixed-pitch blades mounted at four corners of the aircraft [1]. In line with the development of the drone industry and electric passenger cars, there is a new breakthrough in the implementation of quadrotor, where developers are starting to utilize it as a single seat aerial vehicle that is capable to transport people from one location to another, or rather it being called as air taxi [2]. Not limited to that specific course, the vehicle also has been applied in a variety of applications, including surveillance, search and rescue operation and mobile sensor network [1].

A quadcopter can be represented as four motor thrusters on a crossed rigid body and they have similar propeller specification. Basically, their function is to create the airflow that generates the pressure downward and eventually, creating the lift force on the body [3]. The body frame is designed in symmetry to make the quadcopter model more comprehensible.

*Corresponding email: mshariff@utm.my

Generally, the motors are actuated by an electronic speed controller (ESC) and it is controlled by a control board [4]. It is important to understand that in a quadcopter system, the only parameter to be controlled is the speed, which means the trajectory and stability of the quadcopter is controlled by only changing the speed the motors' propeller [3]. From Figure 1, it can be observed that each motor in a quadcopter creates thrust (T) and torque (τ) and the movement of roll, pitch and yaw is determined by varying the motors' speed [3]. The model of the quadrotor is in a right-handed coordinate system and its coordinate frame is represented by (x, y, z) and is referred on the center of the two frames. The frame origin, o_b is at the center of the quadrotor mass and y_b is pointing forward on the quadrotor [5]. In addition, there are four motors denoted by M with different direction of rotation, in which they are positioned in such a way to counter the torque produced by each motor. The movement characteristics of a quadrotor as the results of the changes in the individual motor's speed is depicted in Figure 2.

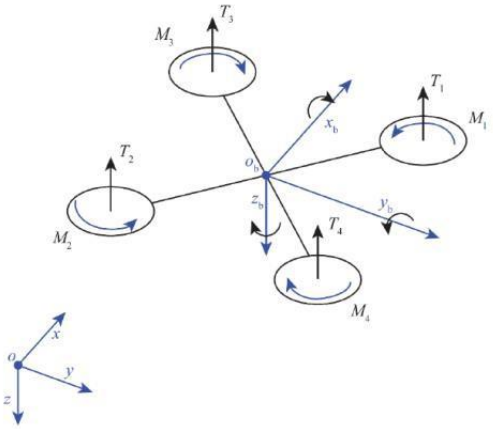

Figure 1: Quadrotor dynamics [5]

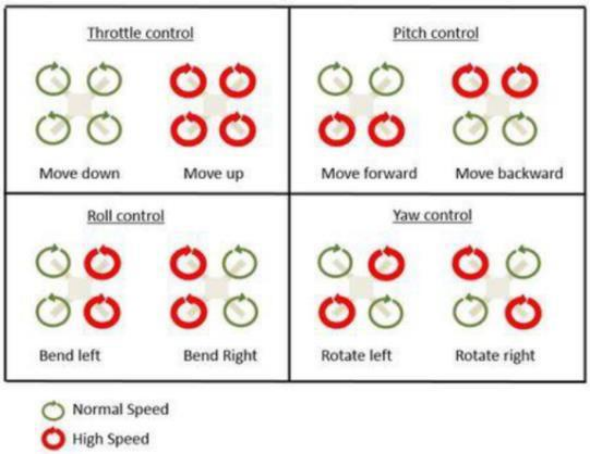

Figure 2: Alternative working principle of a quadrotor [6]

1.1 Commercially Available Manned or Autonomous Aerial Vehicle

In line with the advancement of electric motors, there are few companies who break the barrier of 21st century air transportation by developing and commercialized their very own electrical powered, manned aerial vehicle, as listed in the according subsections. Ehang developed by one of the world's leading tech company of intelligent aerial vehicle [7]. As shown in Figure 3, this particular single seat autonomous aerial vehicle (AAV) uses eight propellers and is operated at low altitude with an objective to solve medium-short distance communication and transportation problems. Moreover, it is designed with full redundancy, which means the vehicle is able to operate normally under unwanted

circumstances. Additionally, this eco-friendly aerial vehicle is installed with *Ehang* fail safe system where it can land automatically at nearest area if one of the components is having failure.

Figure 3: *Ehang 184* AAV [7]

Volocopter 2X is developed by a German company called *Volocopter* and it uses 18 rotors to fly as shown in Figure 4, which make its design very unique, in comparison to other AAVs [8]. It can transport two passengers at one time and completed with redundant systems in all key areas such as propellers, motors and batteries to provide first class safety to passengers. In addition, it utilizes a modern fly-by-light technology in all communication networks and it comes with emergency parachute, in case of accidents.

Figure 4: *Volocopter 2X* [8]

Passenger Drone is a fully AAV and it is designed for two passengers at a time [2]. As shown in Figure 5, it uses 16 engines and propellers and communicated fully by fiber optics or fly-by-light technology. To ensure the safety of customers, *Passenger Drone* is designed to be fool proof, which justify the use of 16 individual rotors. Its dimension is slightly larger than a compact car, which eases the process of transportation and enable it to park in any garage space.

Figure 5: Passenger Drone [2]

2.0 METHODOLOGY

2.1 Design and Modifications

The design and modification processes are divided into three sections; design of the main frame structure, boom and suspension system of the quadcopter. The detailed process of designing in each section is discussed in the subsection sections.

i. Design of the main frame structure

For the main frame, the material is set to be an Aluminum alloy 6061 since it is suitable for aviation purposes and has the lowest density compared to other aviation alloys. The design process is started by determining the specifications of the quadcopter. Then the initial design is drawn in SolidWorks, in which the shape and dimension of pipes (or tubes) are referred to the FURIA helicopter. Based on literature review and consultation, the number of modifications are made and the final design is shown in Figure 6.

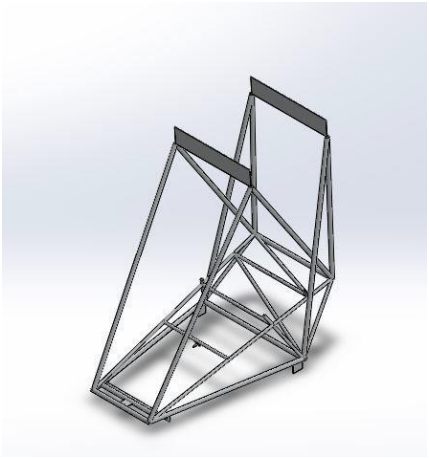

Figure 6: The final design

The main frame is the assembly of the boom, motors and the other related components, as shown in Figure 7. The function of the dome is to store batteries, wiring system, parachute container and other electric components, and it is designed according to the dimension of mentioned items.

Figure 7: The isometric view of assembly design

ii. Design of the boom

The boom is actually a part that holds four motor thrusters, which can be modelled as Figure 8. To ensure that the particular section is stiff enough of its airworthiness and produces low weight at the same time, the minimum thickness of boom was calculated by using bending stress theory. Then, few commercially available models with different outer diameter and thickness, based on the calculation were proposed to be analyzed. The results were then interpreted to choose the best dimension that fits the mentioned requirements.

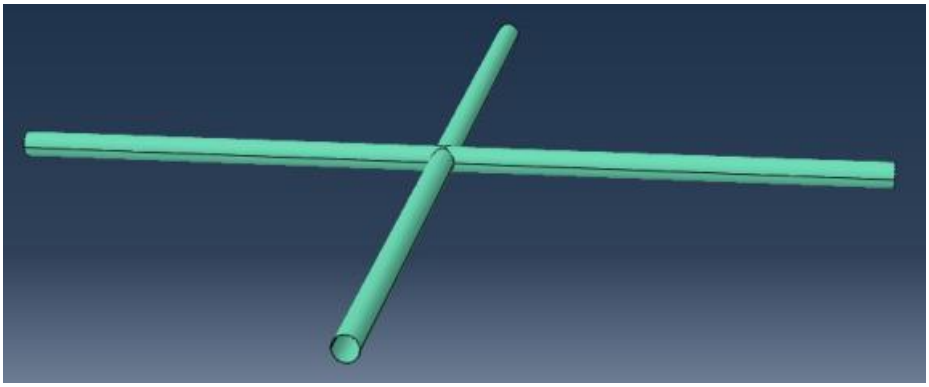

Figure 8: Model of the boom structure

iii. Design of the suspension system

This subsection is focusing on determining the spring and damping constants, *k* and *c*, respectively. By using the critical value of the displacement in the dynamic analysis, the suitable value of *k* and *c* is estimated by using MATLAB and Simulink. The graphs of the displacement against time were plotted to show the damping process and the effectiveness of the suspension system. From the graphs, the best values of *k* and *c* were chosen.

2.2 Weight and Center of Gravity Estimation

The weights of components are obtained through market research. After this particular process, the center of gravity of the quadcopter is then estimated by using SolidWorks and its position acts as a reference to install the boom on the main frame. The location of the center of gravity is indicated roughly in the middle of Figure 9.

Figure 9: The center of gravity of the quadcopter

2.3 Structural Analysis

i. Selection of boom size

Since the boom has symmetry shape with similar forces and boundary conditions at all sides, the model from Figure 8 can be simplified into a model shown in Figure 10. The objective of this analysis is to select the most suitable size of the boom which requires it to support the total weight the aircraft and conserve its own weight at the same time. The size of the boom does matter as the experimental work conducted by Ishak *et al*. [9, 10] had successfully pointed out that the aerodynamic drag characteristics were very sensitive to the helicopter profile. Part of the the problem definitions of the boom structure is shown in Figure 10.

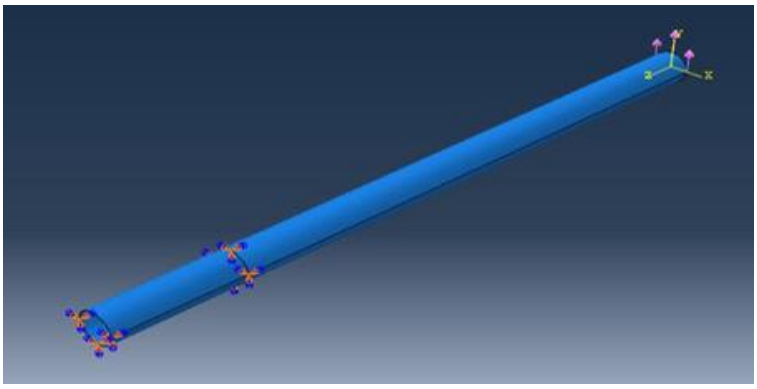

Figure 10: Analysis of different sizes of boom

ii. Analysis of seat support

For this analysis, the whole main frame is imported into *ABAQUS*. The purpose is to determine whether the structure that acts as a seat support is strong enough to withstand an operator or otherwise. For this case, the weight of an operator is distributed on seat support and the base of the frame is fixed, as indicated in Figure 11.

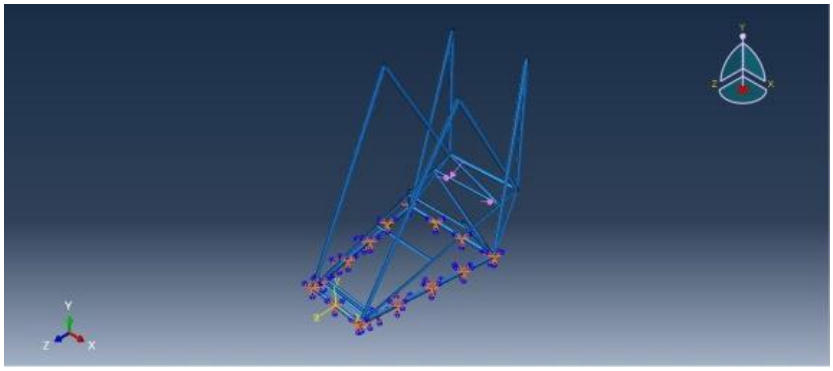

Figure 11: Strength analysis of the seat support

iv. Buckling of column

This analysis was done to find out the critical stress at the attachment points of the main frame and boom, which are the critical parts of the whole structure. In this specific case, the aircraft was assumed to be at rest and the loads are due to the weights of boom and other components above the main frame such as the electric motors, propellers and parachute, which were assumed to be 100 kg. The loads and boundary conditions were defined as shown in Figure 12.

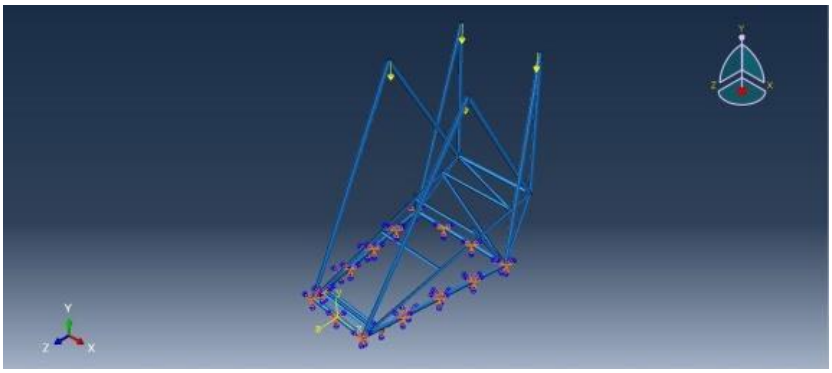

Figure 12: Analysis of buckling of column

v. Analysis of tube during hovering

For this study, the aircraft is assumed to be in hovering state, which means that the thrust is equal to its weight ($T = W$). The graphical representation of the state is illustrated in Figure 13.

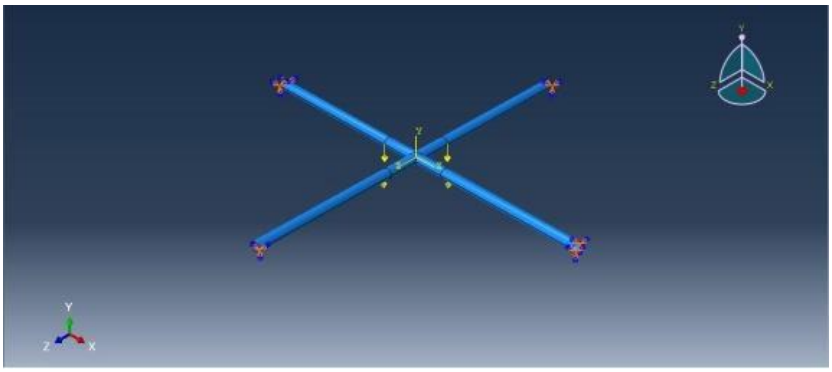

Figure 13: Analysis of tube during hovering

vi. Drop test

The objective of this analysis is to find the safe height of autorotation of the quadrotor. In this analysis, the main frame is dropped at several heights and the impact force is applied

to the critical parts of the structure. To get the worst case, the braking force is assumed to be zero and the height is started at about 6.1 m (20 ft), which is the safe height for the autorotation of a helicopter [11]. For the analysis, two types of materials were used, namely, Aluminum 6061 and Steel 4041. Then the results were compared to determine which material has the highest safe height for autorotation. The value of the maximum stress from the results of all analysis was compared with the allowable stress, which is the tensile yield strength of the material, E = 276 MPa. If the maximum stress is less than this threshold value, the structure is deemed safe under the applied loads.

3.0 RESULTS AND DISCUSSION

3.1 Selection of Boom Size

Works done by Ishak *et. al*. indicate that the helicopter main rotor contributes to the unsteady wake phenomenon [12-14]. Numerical simulation can be considered as a faster and cheaper solution than the wind tunnel testing or other experimental works [15]. Subsequently, the proposed models in this study were analyzed numerically using *ABAQUS*. The results for the stress distribution and deflection of Model 1 are shown in Figures 15 and 16, respectively.

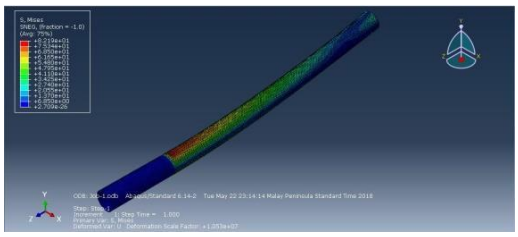

Figure 15: Stress distribution of Model 1

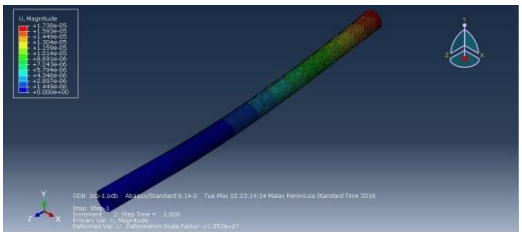

Figure 16: Deflection of Model 1

The maximum stress of each model was compared with the tensile yield strength of the material, i.e., E = 276 MPa. From the results, all the proposed models were regarded safe under the applied loading condition. To conserve the weight, Model 1 is chosen as the boom structure because it has the lowest mass in comparison with the others.

3.2 Analysis of Seat Support

The values of the maximum stress of 0.354 MPa and deflection of 6.932e-9 mm can be derived in Figures 17 and 18, respectively. By comparing the critical stress with the tensile yield strength of the material, the safety factor is definitely more than 1.0, which means that the particular section is safe under the applied load.

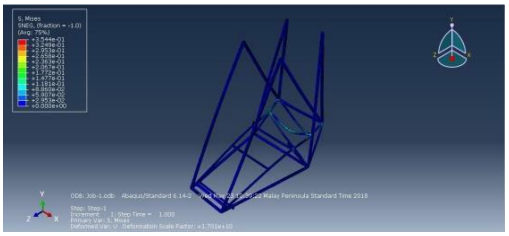

Figure 17: Stress distribution of the seat support

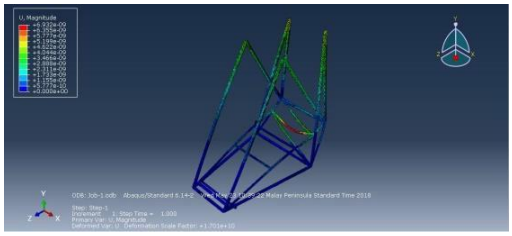

Figure 18: Deflection of seat support

3.3 Buckling of Column

The force in this particular analysis is due to the total weight of boom and other components above the main frame. The values of the maximum stress and deflection are 93.89 MPa and 2.896 e-6 mm, respectively as shown in Figures 19 and 20. In comparison to the material's strength, the calculated safety factor is 2.9, implying that the columns are statically safe.

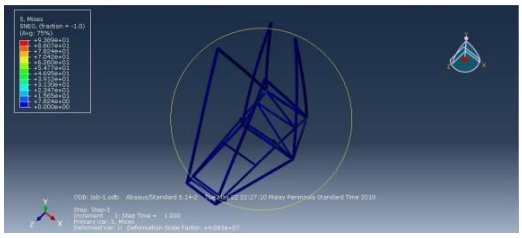

Figure 19: Stress distribution of the main frame

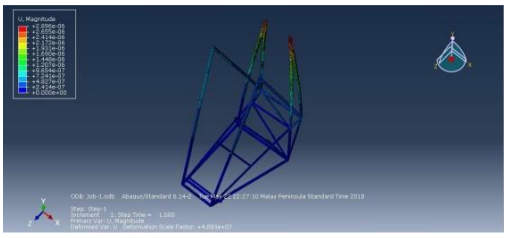

Figure 20: Deflection of the main frame

3.4 Analysis of the Boom During Hover

The results in Figures 21 and 22 show the maximum stress and deflection of the boom when the maximum take-off weight (MTOW) is applied at each of the attachment point are 48.59 MPa and 7.316 e-6 mm, respectively. Similar process of comparison is done in this analysis and the safety factor is computed to be 5.7. This indicates that the boom is structurally safe during hovering when the MTOW is applied at the assigned points.

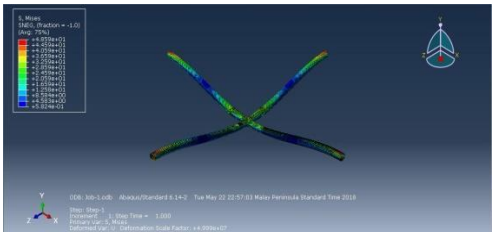

Figure 21: Stress distribution of the boom

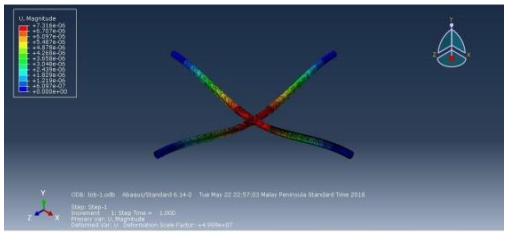

Figure 22: Deflection of the boom

3.5 Drop Test of the Main Frame

The impact force of the assigned heights is calculated and the results are tabulated in Table 1. The total impact force was then divided by the number of attachment points, which is four in this case.

Table 1: Impact force at certain heights

Case	Height (ft)	Height (m)	Velocity (m/s)	Total impact force (kN)
1	20	6.096	10.94	1197
2	10	3.048	7.73	597.5
3	5	1.524	5.47	299.2
4	2.5	0.762	3.87	37.4

i Aluminum 6061

A sample of the results for Aluminum 6061 is shown in Figures 23 and 24. The results for all the four cases are summarized in Table 2.

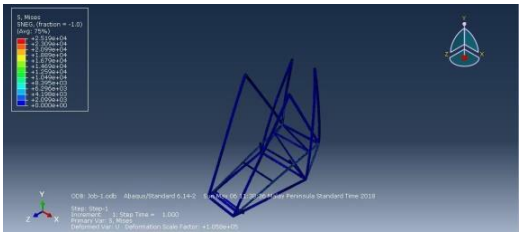

Figure 23: Stress distribution of main frame for Case 1

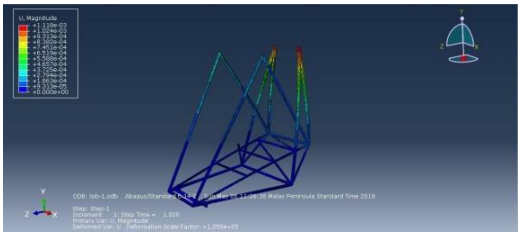

Figure 24: Deflection of main frame for Case 1

Table 2: Results of drop test for Aluminum 6061

Case	Max stress (MPa)	Max deflection (mm)
1	25190	1.183e-3
2	12590	5.888e-4
3	6301	2.796e-4
4	3510	1.398e-4

ii. Steel 4041

The size of steel is based on the FURIA's dimension that is smaller than Aluminum 6061. The same impact forces as given in Table 1 were applied. The results for Case 1 are shown in Figures 25 and 26 and for all the four cases summarized in Table 3.

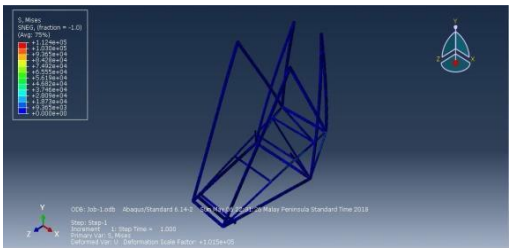

Figure 25: Stress distribution of main frame for Case 1

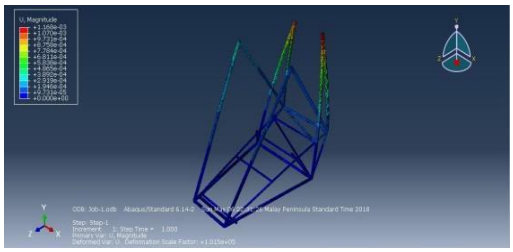

Figure 26: Deflection of main frame for Case 1

Table 3: Results of drop test for Steel 4041

Case	Max stress (MPa)	Max deflection (mm)
1	112500	1.168e-3
2	56270	5.782e-4
3	28150	2.893e-4
4	14080	1.447e-4

As expected, the highest maximum stress and deflection among the cases for both materials is the Case 1, in which the main frame is dropped from the highest drop point (h = 6.096 m). From Tables 2 and 3, the results were used to plot a graph of the maximum stress against the drop height for both materials as shown in Figures 27 and 28. The safe drop height for the frame made from Aluminum 6061 or Steel 4041 can be determined by the value of tensile yield strength shown for the y-axis. For both cases, the safe drop height was approximately found to be 2 m.

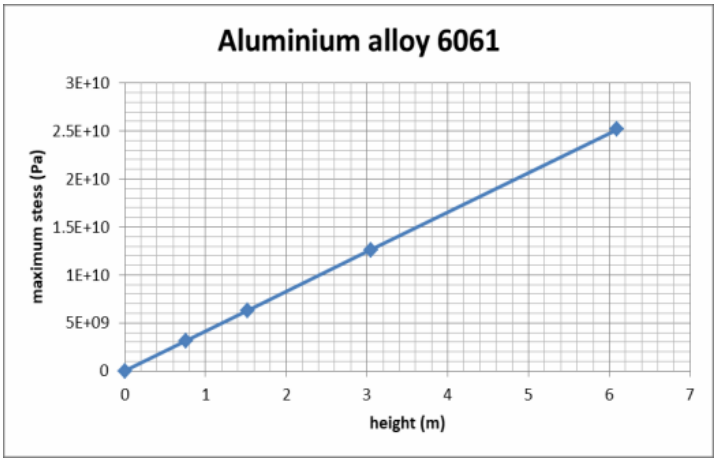

Figure 27: Graph of maximum stress against drop height for Aluminium 6061

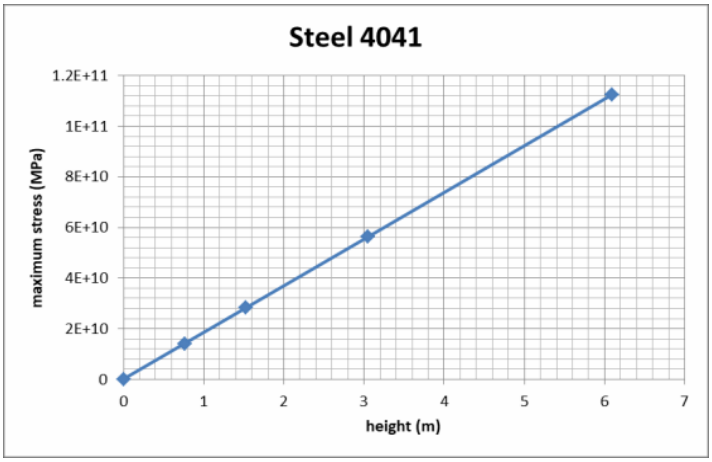

Figure 28: Graph of the maximum stress against drop height for Steel 4041

3.6 Analysis of The Suspension System

The objective of this analysis is to find the suitable value of spring constant, *k* and damping coefficient, *c* for the quadrotor. The transfer functions were derived and represented as a block diagram in MATLAB/Simulink environment as shown in Figure 29. By applying a heuristic trial-and-error method, suitable values of *k* and *c* for the critical displacement (*x*) were determined. After a series of trial runs, a test sample response displayed in Figure 30 shows that the final value of the displacement *x* as time increases is almost zero, implying that the effective values of *k* and *c* are computed as 40000 N/m and 4500 kg/s, respectively through the simulation.

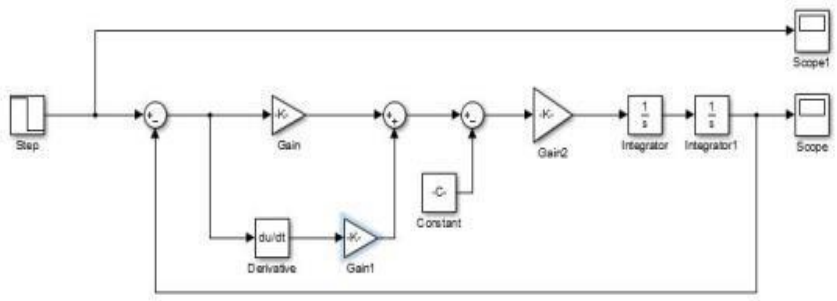

Figure 29: Block diagram in Simulink

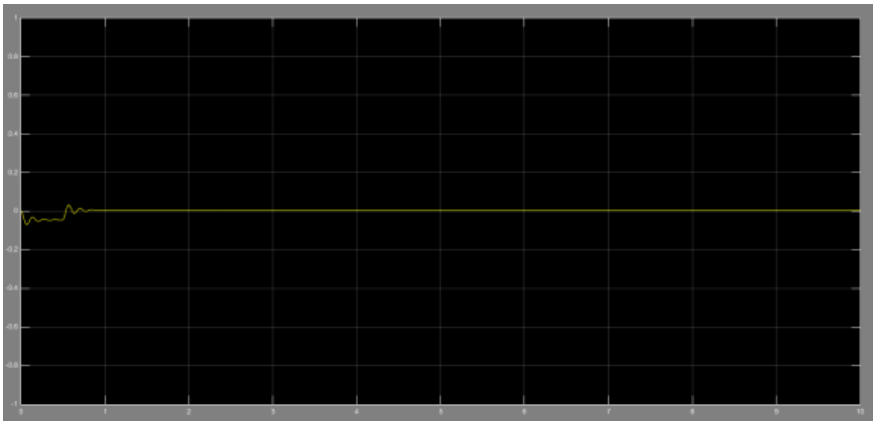

Figure 30: A sample of the system response

4.0 CONCLUSION

The design of the main frame and boom structures were successfully accomplished. The computational analyses done under various loading conditions successfully quantified the safety factors for the boom, seat support and main frame which is well beyond the value of 1.0. Apart from that, the simulation done using MATLAB/Simulink produced suitable values of the spring and damping constants to be used for the suspension system. As for the recommendation to increase the safe height of the main frame, the column is proposed to be fabricated from a stronger material than Aluminum 6061. Also, the cross-section must be constructed sufficiently large but the length of the column needs to be shorter than the proposed design.

ACKNOWLEDGMENTS

The authors would like to thank the Aeronautics Laboratory of the Universiti Teknologi Malaysia (UTM) for providing valuable technical support to conduct this research project. The authors are also indebted to the UTM for supplementing the research funding through the Research University Grant (RUG), Tier 2 (Vote No.: Q.J130000.2624.14J20).

REFERENCES

1. Hoffman G.M., Huang H., Waslander S.L. and Tomlin C.J., 2007. Quadrotor Helicopter Flight Dynamics and Control: Theory and Experiment, *AIAA Guidance, Navigation and Control Conference and Exhibit*, American Institute of Aeronautics and Astronautics, Hilton Head, South Carolina.
2. A new two-seater electric VTOL manned aircraft launches in burgeoning passenger drone industry, https://electrek.co [Accessed: October 2017].
3. Austin R., 2010. *Unmanned Aircraft Systems: UAVs Design, Development and Deployment*, John Wiley & Sons Ltd., UK.
4. Sharif A.M., 2016. *PID Controller for Aerial Photography UAV*, Universiti Teknologi Malaysia.
5. Mustapa M.Z., 2015. Altitude Controller Design for Quadcopter UAV, *Jurnal Teknologi*, 74(1): 181-188
6. Schmidt M.D., 2011. *Simulation and Control of A Quadrotor Unmanned Aerial Vehicle*, Master Thesis, University of Kentucky, USA.
7. Ehang 184, http://www.ehang.com [Accessed: October 2017].
8. Volocopter, https://www.volocopter.com [Accessed: October 2017].
9. Ishak I.S. and Mougamadou Z.M.F., 2017. Effect of Helicopter Horizontal Tail Configurations on Aerodynamic Drag Characteristics, *Jurnal Teknologi*, 79: 67 – 72.
10. Ishak I.S. and Mougamadou Z.M.F., 2017. Experimental Research on Helicopter Horizontal Tail Drag, *The 2nd Multidisciplinary Conference on Mechanical Engineering 2017 – MCME 2017*, Faculty of Mechanical Engineering, Universiti Teknologi Malaysia, Skudai, Malaysia.
11. Layton D.M., 1984. *Helicopter Performance*. Matrix Publisher.
12. Ishak I.S., Mansor S., Tholudin M.L., Rahman M.R.A., 2009. Numerical Analysis of Helicopter Tail Shake Phenomenon: A Preliminary Investigation, *The 2nd International Meeting on Advances in Thermo-Fluids - IMAT'09*, Bogor, Indonesia.
13. Ishak I.S., Mansor S., Tholudin M.L., Rahman M.R.A., 2009. Numerical Analysis of Helicopter Tail Shake Phenomenon: A Preliminary Study on Unsteady Wake, *2nd International Conference on Engineering Technology 2009 - ICET'09*, Kuala Lumpur, Malaysia.
14. Ishak I.S., Mansor S., Tholudin M.L., Rahman M.R.A., 2018. Numerical Studies on Unsteady Helicopter Main-Rotor-Hub Assembly Wake, *Journal of Advanced Research in Fluid Mechanics and Thermal Sciences*, 47(1): 190-200.
15. Dahalan M.N., Suni A.F., Ishak I.S., Nik Mohd N.A.R., Mat S. 2017. Aerodynamic Study of Air Flow over A Curved Fin Rocket, *Journal of Advanced Research in Fluid*

Mechanics and Thermal Sciences, 40 (1): 46-58.